



Research paper

Large compositional differences in the gases released from the Kizildag ophiolitic body (Turkey): Evidences of prevailingly abiogenic origin



Walter D'Alessandro^{a,*}, Galip Yüce^b, Francesco Italiano^a, Sergio Bellomo^a, Ahmet H. Gülbay^c, Didem U. Yasin^c, Antonina Lisa Gagliano^a

^a Istituto Nazionale di Geofisica e Vulcanologia, Sezione di Palermo, Via Ugo La Marfa 153, 90146 Palermo, Italy

^b Hacettepe University, Department of Geological Engineering, Hydrogeology Division, Beytepe, 06800 Ankara, Turkey

^c Eskişehir Osmangazi University, Department of Geological Engineering, Meselik, 26480 Eskişehir, Turkey

ARTICLE INFO

Article history:

Received 16 August 2016

Received in revised form

7 December 2016

Accepted 19 December 2016

Available online 21 December 2016

Keywords:

Gas geochemistry

Serpentinization

Hydrogen

Abiogenic methane

Stable isotopes

ABSTRACT

We investigated the geochemical features of the gases released from the Kizildag ophiolitic complex (Hatay, Turkey). Twenty-three samples both dissolved in hyperalkaline waters and free gases (bubbling gases and dry seeps) were collected. Samples were analysed for their chemical (He, H₂, O₂, N₂, CH₄ and CO₂) and isotopic (He, $\delta^{13}\text{C-CH}_4$, $\delta^2\text{H-CH}_4$, $\delta^2\text{H-H}_2$) composition including the content and C-isotopic composition of C₂ to C₅ alkanes in free gases. Analytical results evidence H₂ production through low-temperature (<80 °C) serpentinization processes and subsequent abiogenic CH₄ production through Fischer-Tropsch-type reactions. In some sample small additions of methane either of microbial or of thermogenic origin can be hypothesized. At one of the sites (Kisecek) a clear fractionation pattern due to microbial methane oxidation leading to strongly enriched isotopic values ($\delta^{13}\text{C} + 15\%$ and $\delta^2\text{H} - 68\%$) and depletion in methane concentrations has been evidenced. At the dry gas seep of Kurtbagi methane flux measurements have been made and a preliminary output estimation of about 1000 kg per year has been obtained.

© 2016 Elsevier Ltd. All rights reserved.

1. Introduction

The Kizildag ophiolitic body crops out in the Hatay region (southern Turkey) (Dilek and Thy, 2009). It belongs to the peri-Arabian ophiolite belt that includes the Troodos (Cyprus), Baër-Bassit (Syria) and Semail (Oman) ophiolites in the eastern Mediterranean region which are the remnants of the Southern Tethys oceanic lithosphere (Sengör and Yilmaz, 1981). The area, seismically very active, is close to the boundary of three tectonic plates (Anatolian, Arabian and African plates) and is characterised by important tectonic lineaments such as the Dead Sea Transform fault and the Karasu Fault which connects the former to the East Anatolian fault system (Mahmoud et al., 2013).

The Cretaceous Kizildag ophiolitic body belongs to the Paleotectonic units of the area (pre-Pliocene basement rocks) overthrust onto the autochthonous pre-Cambrian to Campanian units

and covered by the Campanian-Maastrichtian to Miocene units (Tekeli et al., 1983). The Cretaceous ophiolite and ophiolitic complex have an extensive spatial distribution in the region (~1000 km²) and are made up of ultramafic tectonites, mafic and ultramafic cumulates, gabbros, sheeted dyke complexes, plagiogranites, pillow lavas, bedded cherts and pelagic limestones (Dilek and Thy, 2009).

Ultramafic rocks and their hydration products (serpentinites) represent mantle pieces that have been displaced by geodynamic processes close to the surface where they are exposed to circulating ground- or seawater. Their study received great impulse in recent years, in particular serpentines, because they play an important role in many geological situations. For example, their formation has a strong impact on the rheology of the lithosphere (Hirth and Guillot, 2013), they could play an important role in the C cycle and geological CO₂ sequestration (Power et al., 2013), they often host important ore deposits (Butt and Cluzel, 2013), and are considered as a possible candidate for the origin of life on the Earth or other planetary systems (McCollom and Seewald, 2013).

A distinguishing characteristic of low temperature (<200 °C)

* Corresponding author.

E-mail address: walter.dalessandro@ingv.it (W. D'Alessandro).

serpentinization in ophiolitic aquifers is the strongly alkaline conditions that could be reached in groundwater. Indeed, fluids discharged from active, low-temperature serpentinites have some of the highest pH values (up to > 12) ever recorded in natural systems on Earth (Mottl et al., 2003). Furthermore, groundwater discharged in alkaline springs is typically accompanied by H₂– and CH₄-rich gas, which sometimes bubbles out in the spring water. Rarely is such gas phase emitted from fractures as a dry seep (Etiopie et al., 2011). In many serpentinites, there may also be a diffusive flux of H₂ and CH₄ over a broad area surrounding springs and vents, but these fluxes have only been studied in a few locations (Etiopie et al., 2011).

Barnes et al. (1967), who studied the composition of hyperalkaline springwater discharged from serpentinized ophiolites in California, were the first to recognise the close association of reducing, strongly alkaline fluids with serpentinization. Cipolli et al. (2004) studying the hyperalkaline springs around Genua (Italy) and applying reaction-path modelling described in depth all the reactions taking place and the environmental conditions leading to the particular water composition of hyperalkaline springs. Meanwhile many other similar fluids have been described all around the world, including sites in Canada, Greece, Italy, Japan, Oman, Philippines, Portugal, Spain, Turkey, U.S.A. both on continents and on the ocean floor (Schrenk et al., 2013).

Recently, hyperalkaline springs and a H₂– and CH₄-rich dry gas seep have been identified at the Kizildag ophiolite and a preliminary geochemical description has been done by Yüce et al. (2014).

The present study shows the results of an extended sampling of the gases collected from the hyperalkaline springs (bubbling and dissolved) and dry seep within the Kizildag ophiolitic body (Hatay province, southern Turkey). With respect to the previous work (Yüce et al., 2014) we extended the samplings including three new sites of hyperalkaline springs and collecting samples from more vents within the same group of springs. Furthermore, we increased the measured parameters and performed soil methane flux measurements at the dry gas seep. The results showed a great variability of the gas composition although pointing to a prevailing abiogenic origin.

2. Study area and methods

2.1. Sampling sites

Six groups of hyperalkaline springs and one gas seep have been located in the area and 23 gas samples (dry seeps, bubbling and dissolved gases) were collected and analysed for their chemical and isotopic composition. The geographic position of the sites is shown in Fig. 1 and the coordinates are displayed in Table 1. The gas seep covers an area of about 500 m² and has two main emission points. One of this comes from an outcrop of ophiolitic rocks and the gas when ignited gives flames up to 50 cm high. The hyperalkaline springs have pH between 10.4 and 12.2 and typical Ca-OH composition. Water isotopes (O, ²H and ³H) indicate long hydrologic circuits (Yüce et al., 2014). The groups of springs are all found along creeks in narrow valleys, have low outputs and are characterised by whitish carbonate deposits. Some of them have many small outlets sometimes covering many tens of meters along the creek. Nearly all have at least one spring with a free bubbling gas phase generally with a very sluggish gas flow.

2.2. Sampling and analytical methods

Free bubbling gas samples were taken by an inverted funnel and free gases were collected at dry seeps by inserting a pipe in the soil

and driving the soil gas to the sampling bottle by a syringe and a 3-way valve. All free gas samples were stored in Pyrex bottles with two vacuum stopcocks. Samples for dissolved gas analyses were collected in glass vials sealed underwater.

In the laboratory, the chemical analyses were carried out by gas-chromatography (Perkin Elmer Clarus500 equipped with a double Carboxen 1000 columns, TCD-FID detectors) using argon as the carrier gas. The free gases were directly injected in the gaschromatograph, while dissolved gases were extracted after equilibrium was reached at constant temperature with a host-gas (high-purity argon) injected in the sample bottle. Details on the analytical procedure are reported in Capasso and Inguaggiato (1998) and Liotta and Martelli (2012). Higher hydrocarbons (C₁-C₅) were analysed in the free gas samples using a Shimadzu 14a GC equipped with FID and a packed Chromosorb PAW 80/100 column. The measurement precision was better than ±5% for common gases and ±10% for trace gases such as the alkanes.

The He-isotope ratio in free gas samples was analysed directly from the sample bottles after purification in the high-vacuum inlet line of the mass spectrometer. The isotope composition of dissolved He was analysed by headspace equilibration (Inguaggiato and Rizzo, 2004; Italiano et al., 2014). He and Ne were then cryogenically separated and admitted into mass spectrometers. The ³He/⁴He ratio and ²⁰Ne content were analysed by a GVI Helix SFT mass spectrometer. Helium isotope compositions are given as R/R_A, namely ³He/⁴He of the sample versus the atmospheric ³He/⁴He (R_A = 1.386 × 10⁻⁶). Measured values were corrected for the atmospheric contamination of the sample (R_C/R_A) on the basis of its ⁴He/²⁰Ne ratio (Sano and Wakita, 1985).

Carbon (CH₄, C₂, C₃, nC₄, iC₄, nC₅ and iC₅) and hydrogen (CH₄ and H₂) isotopic compositions were measured using a Thermo TRACE GC and a Thermo GC/C III interfaced to a Delta Plus XP gas source mass spectrometer. ¹³C/¹²C ratios are reported here as δ¹³C values (±0.1‰ for C₁ to C₅) with respect to the V-PDB standard. ¹H/²H ratios are reported here as δ²H values (±2‰ for CH₄ and ±5‰ for H₂) with respect to the V-SMOW standard.

Soil methane flux measurements were made with the accumulation chamber method (Livingston and Hutchinson, 1995; Baciu et al., 2008; D'Alessandro et al., 2009). The flux chamber has a cross-sectional area of 0.03 m² and height of 10 cm. The chamber top has two fixed capillary tubes, one used to collect chamber gas samples and the other used to balance the pressure between inside and outside. Three gas samples were drawn from the headspace in the chamber at fixed intervals after deployment (3, 6 and 9 min). The 20 mL samples were collected using a syringe and injected through a three-way valve and a needle into a 12 mL pre-evacuated sampling vial (Exetainer®, Labco Ltd.). The over-pressured vials were sent to the laboratory for CH₄ analysis with the same method as for free and dissolved gases.

The flux of CH₄ from the soil has been calculated from the rate of concentration increases in the chamber:

$$\Phi = dC/dt \times V/A \quad (1)$$

where Φ is the flux of a gas, V is the volume of air in the chamber (m³), A is the area covered by the chamber (m²), C is the chamber concentration of a gas and dC/dt is the rate of concentration change in the chamber air for each gas. Volumetric concentrations are converted to mass concentrations accounting for atmospheric pressure and temperature measured in the field. Flux values are expressed as mg-CH₄ m⁻² d⁻¹. Positive values indicate fluxes directed from the soil to the atmosphere and negative values indicate flow from the atmosphere into the soil.

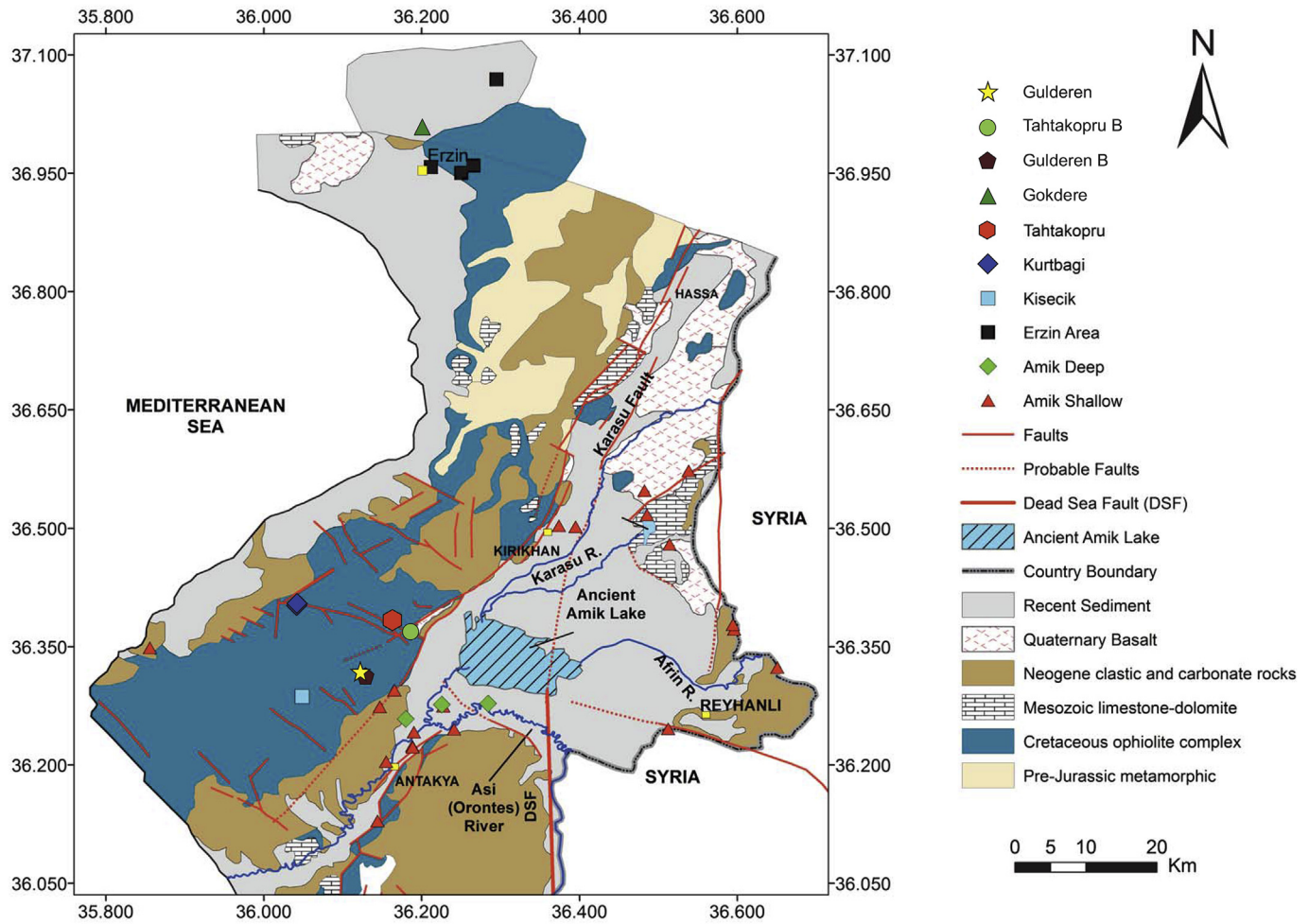


Fig. 1. Simplified geologic map with the sampling points. See Table 1 for sampling sites coordinates.

Table 1
Chemical composition of the gases collected from the Kizildag ophiolite complex.

ID	Site name	Coordinates		Date	He	H ₂	O ₂	N ₂	CH ₄	CO ₂	C ₂	C ₃	C ₄	C ₅	C ₁ /C ₂₊
		Long	Lat												
A23 (*)	Kurtbagi	36.0416	36.4018	05/08/2012	29.0	371,200	1900	25,000	603,800	774	5120	1420	1410	1090	92
A24 (*)	Kurtbagi	36.0429	36.4047	05/08/2012	29.0	384,200	1800	12,600	607,400	983	5090	1390	1290	861	94
A24-2 (*)	Kurtbagi	36.0429	36.4046	27/06/2013	26.0	379,800	5000	21,000	602,900	42	5040	1360	1330	855	94
A24-3	Kurtbagi	36.0429	36.4047	14/09/2014	15.0	180,800	81,800	353,800	390,300	242	3500	989	1020	775	87
A13 (*)	Tahtakopru	36.1636	36.3835	07/08/2012	1.7	487,400	28,500	399,500	102,500	1200	24	11	16	12	2929
A12 (*)	Tahtakopru	36.1636	36.3835	07/08/2012	30.1	499,900	410	380,300	119,300	27	n.d.	n.d.	n.d.	n.d.	–
A12-2 (*)	Tahtakopru	36.1636	36.3835	28/06/2013	4.5	605,000	<200	279,100	120,300	41	30	19	29	25	2455
A12-4	Tahtakopru	36.1636	36.3835	13/05/2014	3.6	277,000	2490	589,900	130,500	54	n.d.	n.d.	n.d.	n.d.	–
A12	Tahtakopru	36.1632	36.3834	14/09/2014	1.6	486,400	32,600	396,600	94,400	<100	40	19	32	26	1600
A12C	Tahtakopru	36.1632	36.3834	14/09/2014	<5	541,600	<200	341,300	121,300	<100	35	15	28	30	2426
A35 (*)	Kisecik	36.0484	36.2869	26/06/2013	7.9	<10	3650	797,300	197,900	1128	n.d.	n.d.	n.d.	n.d.	–
A35-4	Kisecik	36.0484	36.2869	14/05/2014	7.8	<10	18,100	877,300	104,500	88	n.d.	n.d.	n.d.	n.d.	–
A35	Kisecik	36.0484	36.2869	13/09/2014	<5	<10	82,800	841,800	75,400	19	n.d.	n.d.	n.d.	n.d.	–
A45	Kisecik	36.0485	36.2867	13/09/2014	<5	<10	150,800	849,100	36	53	n.d.	n.d.	n.d.	n.d.	–
A45/a	Kisecik	36.0485	36.2867	13/09/2014	<5	<10	4640	995,200	73	102	n.d.	n.d.	n.d.	n.d.	–
A46	Kisecik	36.0485	36.2867	13/09/2014	7.7	<10	37,200	762,500	200,300	15	n.d.	n.d.	n.d.	n.d.	–
A39 (*)	Gulderen	36.1242	36.3159	30/06/2013	40.8	35,000	55,200	621,200	288,600	<20	n.d.	n.d.	n.d.	n.d.	–
A39	Gulderen	36.1242	36.3159	30/06/2013	<5	48,000	250	542,600	397,300	17,000	n.d.	n.d.	n.d.	n.d.	–
A64	Tahtakopru B	36.1865	36.3693	17/09/2014	837	<10	53,400	945,200	300	245	n.d.	n.d.	n.d.	n.d.	–
A69	Gulderen B	36.1292	36.3127	17/09/2014	<5	173,800	19,100	588,100	186,800	<100	69	7	11	12	2458
A69	Gulderen B	36.1292	36.3127	17/09/2014	163	15,180	26,500	772,400	185,500	205	n.d.	n.d.	n.d.	n.d.	–
A71	Gokdere	36.2010	37.0063	18/09/2014	107	<5	78	44,400	941,900	<100	2920	<5	<5	<5	323
A71	Gokdere	36.2010	37.0063	18/09/2014	126	43	122,400	675,000	202,200	265	n.d.	n.d.	n.d.	n.d.	–

IDs in bold refer to free gases (bubbling gases or dry seeps); n.d. = not determined; (*) analysis previously published in Yüce et al., 2014.

3. Results

3.1. Chemical composition

The chemical composition of the analysed samples can be found in Table 1. To allow rapid comparison between free and dissolved gases the latter have been recalculated in $\mu\text{mol mol}^{-1}$ from the obtained partial pressure values. Partial pressure values and dissolved concentrations expressed in $\mu\text{mol L}^{-1}$ are shown as supplementary material in Table S1. All analysed gas species show variations of many orders of magnitude both in the free and in the dissolved gases. Sometimes also the different springs within a group show very different compositions. The dominant gases are always H_2 , CH_4 or N_2 with concentrations ranging from <10 to $605,000 \mu\text{mol mol}^{-1}$, from 36 to $941,900 \mu\text{mol mol}^{-1}$ and from $12,600$ to $995,200 \mu\text{mol mol}^{-1}$ respectively (Fig. 2). Carbon dioxide shows always low concentrations, generally less than $1000 \mu\text{mol mol}^{-1}$. The analysed samples show oxygen concentrations between 78 and $150,800 \mu\text{mol mol}^{-1}$ always lower than atmospheric air values and N_2/O_2 ratios between 4.2 and 2170 always higher than atmospheric air values. Helium shows concentrations between 1.6 and $837 \mu\text{mol mol}^{-1}$. C_2 - C_5 hydrocarbons, determined only on the free gas samples, show concentrations from below detection limit ($5 \mu\text{mol mol}^{-1}$) up to $5120 \mu\text{mol mol}^{-1}$. C_3 - C_5 hydrocarbons in each sample show similar concentrations while C_2 shows 2 to 6 times higher concentrations. All determined hydrocarbons show at least 2 orders of magnitude lower values than methane.

3.2. Isotopic composition

Helium shows R/R_A values ranging from 0.77 to 3.14 (Table 2). The values corrected for atmospheric contamination range from 0.80 to $3.20 R_C/R_A$, however as many samples display $^4\text{He}/^{20}\text{Ne}$ values close to the atmospheric air value (<0.5) their R_C/R_A values have to be treated with caution. Nevertheless, the obtained values align along a mixing trend between atmospheric air and a deep end-member of prevailing crustal origin but with a significant (10 – 20%) mantle contribution (Fig. 3) considering a SCLM-type mantle end-member ($6.5 R/R_A$ - Yüce et al., 2014). Such pattern fits well with the deep end-member defined for most of the dissolved gases in the shallow (<300 m) groundwaters of the nearby Amik Basin (Yüce et al., 2014). On the contrary the sample of Gokdere with a R/R_A value of 3.14 shows a higher (48%) mantle contribution in line with the values measured in the close by thermal waters of the Erzin area (R/R_A values from 2.60 to 4.85 ; TUBITAK, 2015). This area is very close to the East Anatolian Fault which has been demonstrated to be a pathway of mantle fluids towards the earth's surface (Italiano et al., 2013).

The isotopic composition of methane ranges from -30.5%

to $+15.0\%$ for carbon and from -326% to -68% for hydrogen (Table 2). Hydrogen shows $\delta^2\text{H}$ values from -762% to -681% (Table 2). $\delta^{13}\text{C}$ values of C_2 - C_5 hydrocarbons were measured only in two samples giving values from -25.9% to -17.2% (Table 3).

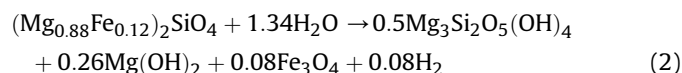
3.3. Soil methane fluxes

Soil methane flux values were measured in 18 sites of the dry seep area. The measurements covered respectively 10 and 8 points of the two main degassing areas. The obtained values span over a very wide range from -11.6 up to more than $10^7 \text{mg m}^{-2} \text{d}^{-1}$ (Table 4). The highest flux value was measured at one of the gas sampling points. Four of the flux measuring sites show negative values which are in the range of dry Mediterranean soils (Castaldi and Fierro, 2005). The remaining sites show values up to $38,100 \text{mg m}^{-2} \text{d}^{-1}$ typical of hydrocarbon prone areas (Etiopie et al., 2008).

4. Discussion

4.1. Hydrogen production through low temperature serpentinization

Fluids containing high levels of H_2 and CH_4 are one of the most distinctive characteristics of rocks undergoing active serpentinization (McCullom and Seewald, 2013). Serpentinites form through the aqueous alteration and hydration of ultramafic rocks predominantly composed of the minerals olivine and pyroxene. Hydrolysis of olivine can result in the formation of molecular hydrogen (H_2) as a result of the oxidation of ferrous iron (Fe(II)) in olivine and the concomitant reduction of water as shown below.



olivine + water \rightarrow serpentine + brucite + magnetite + hydrogen

Usually, ferric iron (Fe(III)) is incorporated into magnetite (Fe_3O_4), brucite ($\text{Mg}(\text{OH})_2$) and/or serpentine minerals ($(\text{Mg,Fe})_3\text{Si}_2\text{O}_5(\text{OH})_4$) depending on activity of Si, water to rock ratios, temperature and compositional differences of the protolith.

Serpentinization processes could occur in a large variety of geodynamic situations from within the mantle up to the shallowest parts of the crust (Evans et al., 2013). Although H_2 formation is thermodynamically favourable over a wide range of temperatures, at low temperatures production rates could be very low. Therefore, most of the laboratory experiments made to study H_2 production in serpentinization processes have been made at temperatures >200 °C (Jin et al., 1999; Seyfried et al., 2007; McCullom and Bach, 2009). Recently Neubeck et al. (2014) demonstrated that H_2 production from alteration of natural olivine sand can be achieved even at 30 °C. At low temperature the catalytic action of accessory minerals and particularly spinels plays an important role in H_2 generation (Mayhew et al., 2013).

Hydrogen generating serpentinization processes can be invoked for the sometimes very high H_2 concentrations found in many on land serpentinization areas as for example in Oman (Neal and Stanger, 1983), Zambales, Philippines (Abrajano et al., 1988), Chimera, Turkey (Etiopie et al., 2011), The Cedars, California (Morrill et al., 2013). The same processes are responsible of the sometimes very high H_2 contents in both the free and dissolved gases of the study area (Fig. 2). As previously pointed out also by Yüce et al. (2014), the very negative $\delta^2\text{H}$ - H_2 values (from -724 to -681%) point to equilibrium temperature of less than 80 °C

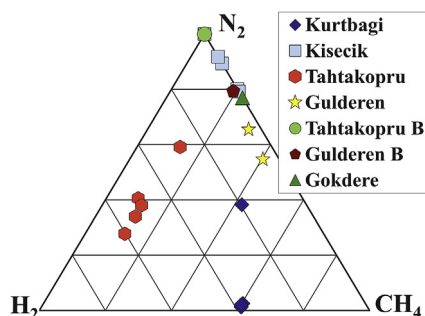


Fig. 2. CH_4 - H_2 - N_2 triangular plot.

Table 2
Isotopic composition of the gases collected from the Kizildag ophiolite complex.

ID	Date	R/R _A	Error	He/Ne	He	Ne	R _C /R _A	δ ¹³ C CH ₄	δ ² H CH ₄	δ ² H H ₂
					μmol mol ⁻¹	μmol mol ⁻¹		‰	‰	‰
					cc L ⁻¹ STP	cc L ⁻¹ STP				
A23 (*)	05/08/2012	1.33	0.006	526	42.8	0.1	1.33	-5.6	-107	-749
A24 (*)	05/08/2012	1.24	0.006	516	35.7	0.1	1.24	-5.1	-103	-762
A24-2 (*)	27/06/2013	1.39	0.007	8.46	29.0	3.4	1.40	-4.8	-96.5	-704
A24-3	14/09/2014	n.d.	n.d.	n.d.	n.d.	n.d.	n.c.	-2.4	-96	-702
A13 (*)	07/08/2012	0.98	0.030	0.311	1.7	5.5	n.c.	-30.5	-326	-745
A12 (*)	07/08/2012	0.98	0.028	3.94	2.41.E-04	6.11.E-05	0.98	n.d.	n.d.	n.d.
A12-2 (*)	28/06/2013	n.d.	n.d.	n.d.	n.d.	n.d.	n.c.	-30.4	-314	-712
A12-4	13/05/2014	0.77	0.050	0.326	4.17.E-05	1.28.E-04	n.c.	-27.8	-304	n.d.
A12	14/09/2014	0.92	0.032	0.331	1.6	4.7	n.c.	-31.9	-325	-724
A35 (*)	26/06/2013	0.99	0.035	0.444	5.02.E-05	1.13.E-04	0.96	n.d.	n.d.	n.d.
A35-4	14/05/2014	0.84	0.050	0.298	5.62.E-05	1.89.E-04	n.c.	-12.6	-296	n.d.
A35	13/09/2014	n.d.	n.d.	n.d.	n.d.	n.d.	n.c.	15.0	-68	n.d.
A46	13/09/2014	0.87	0.012	0.377	5.13.E-05	1.36.E-04	n.c.	-3.6	-265	n.d.
A39 (*)	30/06/2013	0.98	0.030	0.321	5.51.E-05	1.72.E-04	0.86	-16.8	n.d.	n.d.
A64	17/09/2014	0.86	0.017	0.869	6.62.E-05	7.61.E-05	0.80	n.d.	n.d.	n.d.
A69	17/09/2014	n.d.	n.d.	n.d.	n.d.	n.d.	n.c.	-14.4	-324	n.d.
A69	17/09/2014	0.82	0.027	0.959	3.27.E-05	3.41.E-05	0.74	-10.6	-304	-681
A71	18/09/2014	3.14	0.026	12.4	80.7	6.5	3.20	-7.9	-137	n.d.
A71	18/09/2014	n.d.	n.d.	n.d.	n.d.	n.d.	n.c.	-7.5	-137	n.d.

IDs in bold refer to free gases (bubbling gases or dry seeps) and the corresponding He and Ne concentrations are expressed in μmol mol⁻¹; n.d. = not determined; n.c. = not calculated; (*) analysis previously published in Yüce et al., 2014.

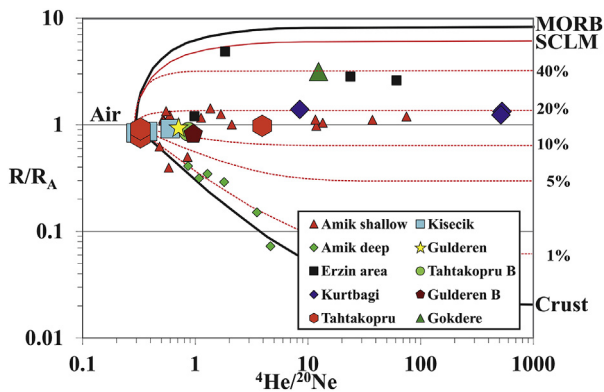


Fig. 3. Helium isotope signature of the collected samples. Data are superimposed on mixing curves (solid lines) of three end-member components, Air, MORB and Crust, for which the assumed typical values are: MORB-type mantle R/R_A = 8 and SCLM mantle R/R_A = 6.5, ⁴He/²⁰Ne > 1000 (red line); crust R/R_A = 0.02 and ⁴He/²⁰Ne > 1000; air R/R_A = 1 and ⁴He/²⁰Ne = 0.318. Further air-crust mixing curves with 1, 5, 10 and 20% of SCLM mantle contribution have also been added (red stippled lines). Amik shallow and deep are from Yüce et al. (2014) and indicate groundwater samples collected from the Amik Plain from springs and shallow boreholes (<500 m) and deep boreholes (>1000 m) respectively. Erzin area refers to springs and boreholes collected close to the town of Erzin (TUBITAK, 2015). The error bars for helium isotopic measurements are within the symbols dimension. (For interpretation of the references to colour in this figure legend, the reader is referred to the web version of this article.)

Table 3
Carbon isotopic composition of C₁ to C₅ alkanes.

Date	C ₁	C ₂	C ₃	nC ₄	nC ₅	isoC ₄	isoC ₅
	δ ¹³ C‰						
A24-3	14/09/2014	-2.4	-17.2	-25.2	-23.9	-25.9	-25.9
A71	18/09/2014	-7.9	-21.9	n.d.	n.d.	n.d.	n.d.

n.d. = not determined.

considering the isotopic geothermometer of Horibe and Craig (1995) between H₂ and H₂O.

Beside samples with very high H₂ contents a lot of samples of

Table 4
Methane fluxes from the soil at the dry gas seep of Kurtbagi.

Site	CH ₄
	mg m ⁻² d ⁻¹
KU01	4.5
KU02	-3.1
KU03	109
KU04	2100
KU05	20.1
KU06	118
KU07	114
KU08	12.5
KU09	-1.3
KU10	-1.3
KU11	1.7
KU12	38,100
KU13	3360
KU14	3600
KU15	-11.6
KU16	11,900
KU17	3160
KU18	13,580,000

the Kizildag ophiolite show low to very low (even below detection limit) concentrations. These low values may be due to H₂ con-

sumption by Fisher-Tropsch-type reactions as shown in more detail in the next paragraph or by microbial utilization (McCullom, 2007). Such processes are responsible of the H₂-depletion trend on Fig. 4.

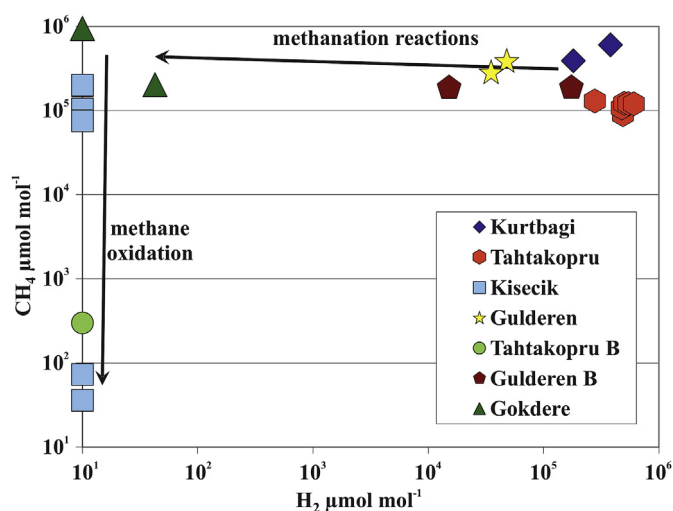
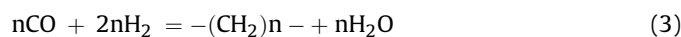


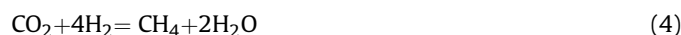
Fig. 4. H_2 vs. CH_4 binary plot. The arrow indicates the compositional changes due to the methane formation through Fischer-Tropsch-type reactions (methanation) and the methane consumption through microbial oxidation.

4.2. Origin of methane

The presence of abundant H_2 in serpentinization environments favours the inorganic production of methane and higher hydrocarbons by Fischer-Tropsch-type reactions (Etiopie and Sherwood-Lollar, 2013). They comprise the Fischer-Tropsch reaction sensu stricto, which refers to the catalytic hydrogenation of carbon monoxide (CO) to produce a wide range of linear, long-chain hydrocarbons:



and the Sabatier reaction (methanation).



It is assumed that Fischer-Tropsch reactions account for most of the methane produced in serpentinization environments although some other reactions have been proposed (Etiopie and Sherwood-Lollar, 2013) including also the direct formation of methane from serpentinization reactions (Suda et al., 2014).

It was previously assumed that Fischer-Tropsch reactions could produce significant amounts of methane only at high temperatures (>200 °C) but recently Etiopie and Ionescu (2015) demonstrated that in the presence of Ruthenium, an element generally present in chromite ores within ophiolitic sequences, the methanation reactions proceed at sufficient rate also at low temperature (20–90 °C). Concordantly chromite outcrops have been found also at the Kizildag ophiolite complex (Dilek and Thy, 2009) and there is abandoned chromite mine in the area of Kurtbagi.

The binary diagram $\delta^{13}C$ vs. δ^2H , called “Schoell diagram” (Schoell, 1980), has been used for the classification of the origin of methane in natural gas mixtures. It has recently been updated to account for methane of abiogenic origin (Etiopie and Schoell, 2014). In the Schoell diagram (Fig. 5) the gases of Kizildag ophiolite are compared to gases of other ophiolitic systems. Some of the sampled gases (Kurtbagi and Gokdere) display δ^2H and $\delta^{13}C$ values which are considered typical of abiogenic methane. The measured range (–7.9 to –2.4‰ and –137 to –96‰ respectively – Fig. 5) is similar to the most studied type-localities of low-temperature serpentinization like Zambales, Philippines (Abrajano et al., 1988), Chimera, Turkey (Etiopie et al., 2011) and the ocean bottom site of Lost City (Proskurowski et al., 2008).

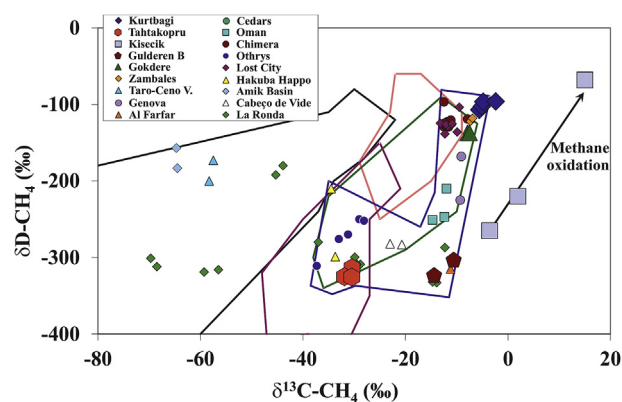


Fig. 5. $\delta^{13}C$ vs. δ^2H binary diagram (Schoell diagram). The plotted fields are from Etiopie and Schoell (2014), black line = biogenic; brown line = Precambrian crystalline rocks; green line = serpentinized systems; orange line = volcanic/hydrothermal systems, and from Etiopie et al. (2015), blue line = land-based serpentinization. The arrow evidences the isotopic fractionation due to microbial oxidation of methane. Samples from the Kizildag ophiolite are compared with literature data from other serpentinization areas. (Hakuba Happo – Japan, Suda et al., 2014; Oman, Fritz et al., 1992; Cedars – California, Morrill et al., 2013; Chimera – Turkey, Etiopie et al., 2011; Zambales – Philippines, Abrajano et al., 1988; Othrys – Greece, Etiopie et al., 2013a; Taro and Ceno Valleys – Italy, Boschetti et al., 2013a; Lost City – Atlantic Ocean, Proskurowski et al., 2008; Genova – Italy, Boschetti et al., 2013b; Cabeco da Vide – Portugal, Etiopie et al., 2013b; Al Farfar – U.A.E. Etiopie et al., 2015; La Ronda – Spain, Etiopie et al., 2016). The two samples called Amik Basin refer to dissolved methane in a 1270 m deep borehole in the Amik Basin (Yüce et al., 2014). (For interpretation of the references to colour in this figure legend, the reader is referred to the web version of this article.)

Methane of other sites (Tahtakopru, Gulderen and Gulderen B) shows more negative values especially for δ^2H . Etiopie and co-workers (Etiopie and Sherwood-Lollar, 2013; Etiopie and Schoell, 2014) recently suggested that such values could be also considered of abiogenic origin. Further studies of Etiopie and co-workers (Etiopie et al., 2015, 2016) expanded the field of methane isotopic values of land based serpentinization areas towards positive $\delta^{13}C$ values coupled with very negative δ^2H values. Such expansion fits well with the values measured at Gulderen B.

The samples collected in the area of Kisecik display variable values which are aligned along a methane oxidation trend. The sample least affected by oxidation processes still plots close to the field defined by Etiopie et al. (2015). The slope of isotopic enrichment for the Kisecik samples, calculated as $\delta^2H/\delta^{13}C$ (10.8), is within the slope of oxidation predicted by previous experimental studies with methanotrophs, which range from 5.9 to 13 (Cadieux et al., 2016 and references therein). Methanotrophs are microorganisms that use methane as their energy and C source (Hanson and Hanson, 1996). Preliminary microbiological investigations assessed the presence of methanotrophic microorganisms in some of the waters of the Kizildag area including Kisecik (Quatrini et al., 2016). Although methanotrophic microorganisms have been discovered also in other serpentinization area, as for example at Cabeco da Vide, Portugal (Tiago and Veríssimo, 2013) and at Santa Elena ophiolite, Costa Rica (Sanchez-Murillo et al., 2014), isotopic fractionation of methane due to microbial activity has not been described until recent times in hyperalkaline waters. Such fractionation has been hypothesized in the serpentinites in Oman (Miller et al., 2016) where methanotrophs have also been discovered and $\delta^{13}C-CH_4$ reaches values up to +3‰ while δ^2H-CH_4 remains quite negative (–205‰). At Kisecik the strong isotopic fractionation (up to +15‰ for $\delta^{13}C$ and –68‰ for δ^2H) could indicate that a large fraction of the original methane has been oxidized by microbiological activity and could justify the sometimes very low methane concentrations (methanotrophic trend in Fig. 5).

Some of the Kisecek samples have methane concentration too low to allow measurement of its isotopic composition but it could be hypothesized that they have extremely fractionated $\delta^2\text{H}$ and $\delta^{13}\text{C}$ values. Considering that extreme isotopic fractionation due to microbiological activity has been found in many extreme environments like Arctic lakes (Cadieux et al., 2016) and hydrothermal fluids (D'Alessandro et al., 2014; Daskalopoulou et al., 2016) this testifies for the extreme adaptability of methanotrophic microorganisms.

The more negative $\delta^{13}\text{C}\text{-CH}_4$ values measured in the samples collected at Tahtakopru could indicate a small contribution from microbial activity. These springs discharge fluids still very rich in H_2 which could be used by methanogens in the shallowest part of the hydrologic circuit to produce methane. Contribution of microbial methane has been hypothesized in other serpentinizing bodies like Taro and Ceno Valleys (Boschetti et al., 2013a), La Ronda (Etiopie et al., 2016) and The Cedars (Morrill et al., 2013). In the first case the authors suggest that the methane of microbiologic origin derives from the sediments below the ophiolites in the last case methanogens have been identified in the sampled springs suggesting a possible contribution of methane microbiologically produced in the shallowest part of the circuit. In the case of Tahtakopru a contribution of methane from the sediments below the ophiolitic sequence could be possible although probably dominated by thermogenic methane (see next section). Also a contribution of methanogens within the spring water cannot be excluded because the necessary anoxic conditions are often met. Until now such microorganisms have not been identified (analyses still underway) so that the possible microbial methane contribution at Tahtakopru remains speculative.

4.3. Origin of higher hydrocarbons

In principle, Fisher-Tropsch-type reactions can result in the abiogenic synthesis of multiple gaseous hydrocarbons, from ethane to butane, and liquid hydrocarbons (starting from pentane), due to polymerization of CH_4 molecules, methylene ($-\text{CH}_2$), or methyl radicals ($-\text{CH}_3$) in a chain growth sequence (McCullom and Seewald, 2013). Higher hydrocarbons ($\text{C}_2\text{-C}_5$) have been found in many serpentinization sites and their chemical and isotopic composition has been used to unravel the origin of the released gases (Sherwood Lollar et al., 2008; Etiopie et al., 2011; Fiebig et al., 2015).

In the area of the Kizildag ophiolite higher hydrocarbons ($\text{C}_2\text{-C}_5$) have been analysed only in the gases of four sites. In a Bernard graph (Bernard et al., 1976, Fig. 6) all these samples plot outside the areas typical of gases either of thermogenic or microbial origin. But while Kurtbagi and Gokdere show relatively low C_1/C_{2+} ratios from 87 to 323, Tahtakopru and Gulderen B display much higher values (C_1/C_{2+} from 1600 to 2929). Although experimental data suggest that the C_1/C_{2+} ratio of abiogenic gas should be around 45 or less (Morrill et al., 2013 and references therein) most of the gases collected in serpentinization environment display generally values in excess of 100 (Fig. 6). Only few show values < 45 and for some of them (Tableland – Szponar et al., 2013) a contamination by thermogenic gases has been hypothesized. Samples with high C_1/C_{2+} ratios and very low $\delta^{13}\text{C}\text{-CH}_4$ values clearly point towards a contamination by gases of microbial origin (The Cedars – Morrill et al., 2013; Taro and Ceno Valleys – Boschetti et al., 2013a; some of the samples of La Ronda ophiolite – Etiopie et al., 2016). On the other hand some sample considered of pure or prevailing abiogenic origin show C_1/C_{2+} ratios >500 (up to 18,500) with $\delta^{13}\text{C}\text{-CH}_4$ values > -15‰ (La Ronda – Etiopie et al., 2016; Lost City – Proskurowski et al., 2008, Fig. 6). Basing on similarities with other serpentinization systems we can hypothesize that the gases of

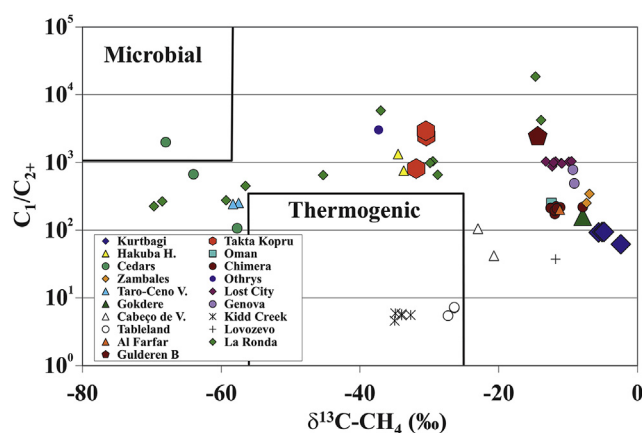


Fig. 6. $\delta^{13}\text{C}\text{-CH}_4$ vs. $\text{C}_1/[\text{C}_2+\text{C}_3]$ ratio binary diagram (Bernard diagram). Samples from the Kizildag ophiolite are compared with literature data from other serpentinization areas. (Hakuba Happo – Japan, Suda et al., 2014; Oman, Fritz et al., 1992; Cedars – California, Morrill et al., 2013; Chimera – Turkey, Etiopie et al., 2011; Zambales – Philippine, Abrajano et al., 1988; Othrys – Greece, Etiopie et al., 2013a; Taro and Ceno Valleys – Italy, Boschetti et al., 2013a; Lost City – Atlantic Ocean, Proskurowski et al., 2008; Genova – Italy, Boschetti et al., 2013b; Cabeco da Vide – Portugal, Etiopie et al., 2013b; Kidd Creek – Canada, Sherwood Lollar et al., 2008; Tableland – Canada, Szponar et al., 2013; Lovozovo – Russia, Potter et al., 2004; Al Farfar – U.A.E. Etiopie et al., 2015; La Ronda – Spain, Etiopie et al., 2016).

Gulderen B are almost totally abiogenic while those of Tahtakopru fit a mixing trend with biogenic gases.

The C-isotope composition of $\text{C}_2\text{-C}_5$ hydrocarbons at Kurtbagi and Gokdere are plotted in Fig. 7a together with literature data. As generally observed for abiogenic gases $\delta^{13}\text{C}$ values of higher HC show lower values with respect to methane. The decreasing trend with increasing carbon number has been explained with lower reactivity of ^{13}C during polymerization processes (DesMarais et al., 1981) leading to the formation of higher hydrocarbons from methane through abiogenic reactions. This trend, shown in Fig. 7a as “spark discharge”, is opposite to typical thermogenic gases where higher hydrocarbons have increasingly higher $\delta^{13}\text{C}$ values (“thermogenic” in Fig. 7a). In this case the isotopic trend is attributed to kinetic isotopic effects where the alkyl groups cleave from the source organic matter. The weaker $^{12}\text{C}\text{-}^{12}\text{C}$ bonds will break at a faster rate than the heavier $^{12}\text{C}\text{-}^{13}\text{C}$ bond leaving residual alkanes more enriched in the ^{13}C with increasing molecular mass (DesMarais et al., 1981). All data in Fig. 7a show coherently a lower C-isotopic of ethane with respect to methane as expected from abiogenic polymerization processes but evidencing otherwise some differences. For example, the two samples from Kizildag show a difference between methane and ethane of about 15‰ while most of the literature data show differences of less than 4‰. The only sample showing a similar difference is that of Chimera and also the laboratory experiment (spark discharge) of DesMarais et al. (1981). Furthermore, in all of the samples the decreasing isotopic trend with increasing carbon number becomes inverted at least since C_4 . Such inversion, found also in the sample of Kurtbagi (in the sample Gokdere $\text{C}_3\text{-C}_5$ HC were to low for isotope measurements), has been explained in different ways. For example, Sherwood Lollar et al. (2008) explained the pattern of Kidd Creek samples assuming rapid abiogenic polymerized chain growth in which carbon isotope fractionation in the formation of C_{2+} compounds is negligible with respect to simple isotopic mass balance. Other authors explained the inverse trend, especially if it does not involve C_2 , as due to small contaminations from thermogenic gases (Etiopie et al., 2011; Szponar et al., 2013).

The evaluation of the Schulz-Flory distribution of a hydrocarbon

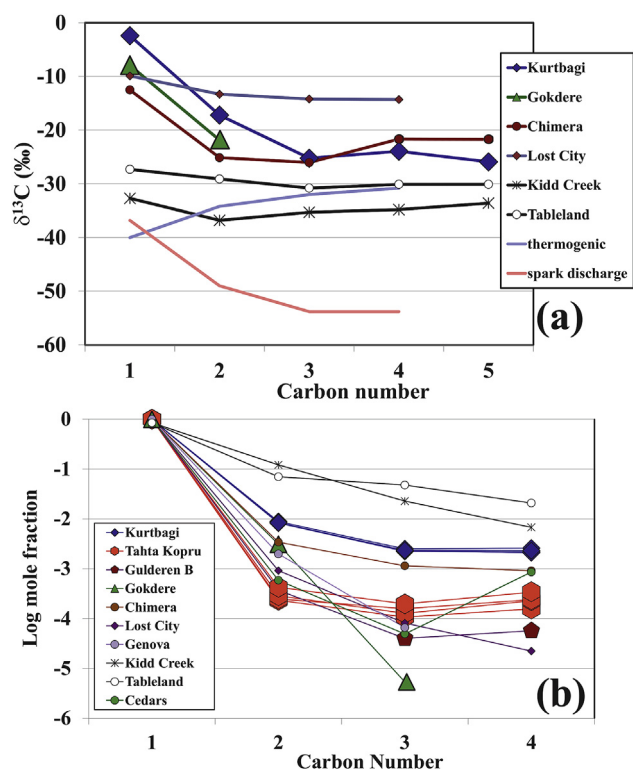


Fig. 7. (a) Plot of ^{13}C sequence of $\text{C}_1\text{--}\text{C}_5$ alkanes and (b) Schulz-Flory distribution of Kizildag ophiolite gases compared with other abiogenic gases (Chimera – Turkey, [Etioppe et al., 2011](#); Lost City, [Proskurowski et al., 2008](#); Genova – Italy, [Boschetti et al., 2013b](#); Kidd Creek – Canada, [Sherwood Lollar et al., 2008](#); Tableland – Canada, [Szponar et al., 2013](#); Cedars – California, [Morrill et al., 2013](#)). The patterns of thermogenic and spark discharge in (a) are taken from [DesMarais et al. \(1981\)](#).

mixture is another indicator used to evaluate the abiogenic origin of the gases (Fig. 7b). [Etioppe and Sherwood-Lollar \(2013\)](#) believe that pure abiogenic gases should display distribution coefficients (r^2) >0.99 while prevalingly abiogenic mixture should have $r^2 > 0.9$. Basing on such classification in the Kizildag area only sample Gokdere ($r^2 = 0.999$) should be considered purely abiogenic. All other samples of Kizildag show very low r^2 values (<0.8) indicating some secondary process that changes the original distribution. Indeed, the statement of [Etioppe and Sherwood-Lollar \(2013\)](#) indicating that prevalingly abiogenic mixture should have $r^2 > 0.9$ is probably far from reality. For example, samples from Lost City and Chimera, for which a prevalingly abiogenic origin has been demonstrated on other basis, display $r^2 < 0.8$. For example, the Chimera sample, which is in many aspects very close to the Kurtbagi sample at Kizildag, for [Etioppe et al. \(2011\)](#) has a prevailing abiogenic origin with a contribution of thermogenic gas estimated in 10–20%. In the case of Chimera the possible source rocks below the ophiolitic sequence have been characterised in their hydrocarbon generating potential. Also beneath the Kizildag ophiolite hydrocarbon source rocks of the Arabian carbonate platform have been identified ([Dilek and Thy, 2009](#)) confirming possible small thermogenic contributions to the Kurtbagi samples.

4.4. Methane output estimate

Fluxes of abiogenic methane in continental serpentinization areas have been measured only since a few years mainly by [Etioppe](#) and co-workers ([Etioppe et al., 2011, 2013a; 2016](#)). Apart from focussed degassing points (eternal flames or bubbling gases) displaying fluxes in excess of $10^5 \text{ mg m}^{-2} \text{ d}^{-1}$, measured values

generally span over flux values ($10^1\text{--}10^3 \text{ mg m}^{-2} \text{ d}^{-1}$) similar to microseepage in hydrocarbon fields ([Etioppe and Klusmann, 2010](#)). A similar situation can be recognised also at the two sites at Kurtbagi. Here a very high flux value of $1.4 \times 10^7 \text{ mg m}^{-2} \text{ d}^{-1}$, corresponding to the main emission point of one of the two areas, has been measured. Similar high flux point sources are present also in the other site but due to the fact that they are issuing from fractures within hard rock (Fig. 8) no flux measurement could be made. Around these point sources microseepage could be evidenced up to distances of 10–20 m. At greater distances only negative flux values were detected indicating that methane was absorbed from the atmosphere by normal methanotrophic activity within the soil profile ([Castaldi and Fierro, 2005](#)).

Basing on these measurements a preliminary estimate of the total methane output has been made. The output of the areas around the main emission points can be estimated multiplying the respectively median flux value by the estimated emission area. Considering median flux values of 110 and $3500 \text{ mg m}^{-2} \text{ d}^{-1}$ and areas of about 300 and 200 m^2 respectively we obtain output values of 13 and 250 kg per year for the two areas. The output of one of the main emission points is easily obtained multiplying the flux value by the surface of the accumulation chamber (0.03 m^2) obtaining an output of at least 150 kg per year. For the other main emission point a rough estimate could be obtained by the height of the burning flame. A flame of at least 40 cm height was present in all occasions we visited the area. [Hosgormez et al. \(2008\)](#), on the basis of fire dynamics models ([Delichatsios, 1990](#)), estimated methane fluxes for a similar natural methane seep at Chimaera (Turkey). For flame heights of 40 cm they estimated outputs in excess of 2000 kg per year. Such value is probably overestimated in the present case because they considered a circular flame diameter at its base $\geq 5 \text{ cm}$. Due to the fact that the flame at Kurtbagi comes from fractures within hard rock a smaller and linear geometry should be considered leading to lower output values. Considering also a few smaller flames ($\leq 15 \text{ cm}$) a reasonable estimate for these point sources would be $\sim 500 \text{ kg per year}$. Summing up, the total output from the soil to the atmosphere of the Kurtbagi area is in the order of about 1000 kg per year.

5. Conclusions

The wide range of chemical composition displayed by the free (bubbling gases and dry seeps) and dissolved gases released from the Kizildag ophiolitic complex encompasses nearly the entire spectrum of gas composition found in serpentinization areas worldwide. Such range points to primary gas production through serpentinization processes at different stages and to a lesser degree to secondary processes (mixing with gases originating outside the ophiolitic body and microbial methane production or oxidation).

The hydrogen-dominated gases derive from the serpentinization of the olivine-rich ultrabasic rocks of the Kizildag ophiolites and the very negative $\delta^2\text{H}\text{-H}_2$ values (from -724 to -681‰) indicate that the serpentinization occurs at low temperatures ($<80 \text{ °C}$).

The $\delta^{13}\text{C}\text{-CH}_4$ values and C_1/C_{2+} ratios measured in the gases collected in the Kizildag area indicate that methane mainly originates from Fischer-Tropsch-type reactions which in active serpentinization areas consume the produced hydrogen reacting with CO_2 of different origins (atmospheric, biological production within soils or geogenic). The more negative $\delta^{13}\text{C}\text{-CH}_4$ values and higher C_1/C_{2+} ratios measured at the Tahtakoprü site, although still compatible with a pure abiogenic origin ([Etioppe and Sherwood Lollar, 2013](#)), could suggest the addition of methane of microbial origin. The sedimentary rocks below the ophiolitic body are an unlikely source of microbial methane. Instead the high concentration of H_2 and the anoxic conditions could suggest that methanogens produce

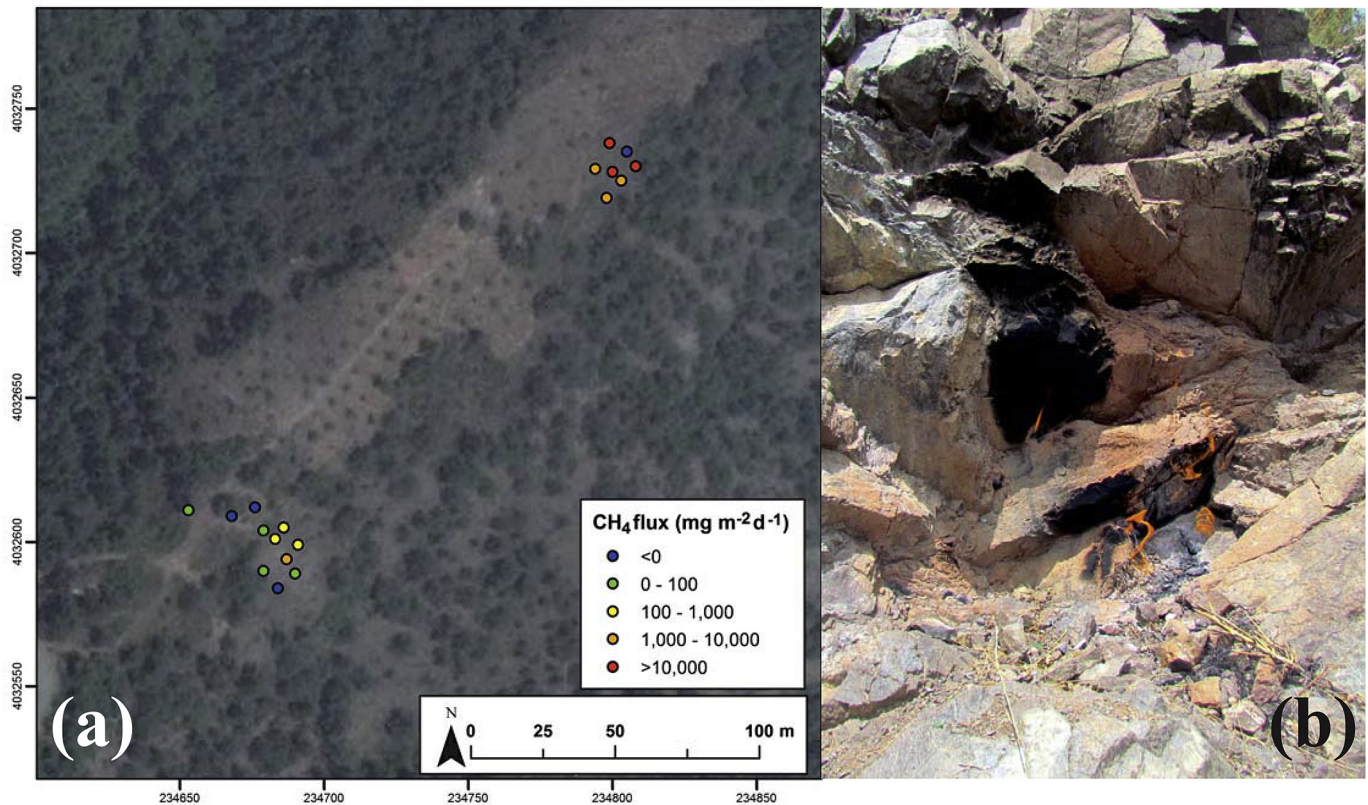


Fig. 8. (a) map of the CH₄ flux measurements made at Kurtbagi Source: “Kurtbagi” 36.4019°N and 36.0415°E. Google Earth. October 1, 2014. August 2, 2016. (b) Picture of the flames issuing from the ophiolitic rocks at one of the sites of Kurtbagi (photo W. D'Alessandro).

methane in the shallowest part of the hydrologic circuit of these springs. Nevertheless, the presence of such microorganisms has still to be proven.

On the contrary microbiologic analyses (Quatrini et al., 2016) evidenced the presence of methanotrophic microorganisms in the Kisecik springs. Biological methane consumption in these springs justifies both the sometimes very low methane concentrations (range from 36 to 200,300 $\mu\text{mol}/\text{mol}^{-1}$) and the very positive $\delta^{13}\text{C}\text{-CH}_4$ and $\delta^2\text{H}\text{-CH}_4$ values aligned along a microbial fractionation line. Although methanotrophic microorganisms have been found also in other hyperalkaline springs this is the strongest fractionation due to microbial activity that has been described in a serpentinization area until now.

Data on concentration and C-isotopic composition of C₂ to C₅ alkanes confirm the prevailing abiogenic origin of the gases and suggest small additions of thermogenic gases.

Finally, a preliminary methane output from the dry seep of Kurtbagi has been estimated in about 1000 kg per year.

Acknowledgements

This work has been funded by the Scientific and Technological Research Council of Turkey (TUBITAK) with the project (COST) no 111Y090. All analyses were made at the laboratories of the INGV of Palermo and we are grateful to all the laboratories responsible and technicians: F. Grassa, M. Martelli, Y. Oliveri, A. Rizzo, F. Salerno, A. Sollami and M. Tantillo. The insightful comments of two anonymous referees helped us to improve the manuscript.

Appendix A. Supplementary data

Supplementary data related to this article can be found at <http://dx.doi.org/10.1016/j.marpetgeo.2016.12.017>.

References

- Abrajano, T.A., Sturchio, N.C., Bohlke, J.K., Lyon, G.L., Poreda, R.J., Stevens, C.M., 1988. Methane-hydrogen gas seeps, Zambales Ophiolite, Philippines: deep or shallow origin? *Chem. Geol.* 71, 211–222. [http://dx.doi.org/10.1016/0009-2541\(88\)90116-7](http://dx.doi.org/10.1016/0009-2541(88)90116-7).
- Baciu, C., Etiopie, G., Cuna, S., Spulber, L., 2008. Methane seepage in an urban development area (Bacau, Romania): origin, extent, and hazard. *Geofluids* 8, 311–320. <http://dx.doi.org/10.1111/j.1468-8123.2008.00228.x>.
- Barnes, I., LaMarche, V.C., Himmelberg, G., 1967. Geochemical evidence of present-day serpentinization. *Science* 156, 830–832.
- Bernard, B.B., Brooks, J.M., Sackett, W.M., 1976. Natural gas seepage in the gulf of Mexico: Earth planet. Sci. Lett. 31, 48–54. [http://dx.doi.org/10.1016/0012-821X\(76\)90095-9](http://dx.doi.org/10.1016/0012-821X(76)90095-9).
- Boschetti, T., Etiopie, G., Pennisi, M., Romain, M., Toscani, L., 2013a. Boron, lithium and methane isotope composition of hyperalkaline waters (Northern Apennines, Italy): terrestrial serpentinization or mixing with brine? *Appl. Geochem* 32, 17–25.
- Boschetti, T., Etiopie, G., Toscani, L., 2013b. Abiotic methane in the hyperalkaline springs of Genova, Italy. *Procedia Earth Plan. Sci.* 7, 248–251. <http://dx.doi.org/10.1016/j.proeps.2013.02.004>.
- Butt, C.R.M., Cluzel, D., 2013. Nickel laterite ore deposits: Weathered serpentinites. In: *Serpentines* (Guillot, S., Hattori, K., eds.), *Elements* 9(2), 123–128. doi: 10.2113/gselements.9.2.123.
- Cadioux, S.B., White, J.R., Sauer, P.E., Peng, Y., Goldman, A.E., Pratt, L.M., 2016. Large fractionations of C and H isotopes related to methane oxidation in Arctic lakes. *Geochim. Cosmochim. Acta* 187, 141–155.
- Capasso, G., Inguaggiato, S., 1998. A simple method for the determination of dissolved gases in natural waters. *Appl. Therm. waters Vulcano Isl. Appl. Geochem* 13, 631–642.
- Castaldi, S., Fierro, A., 2005. Soil – atmosphere methane exchange in undisturbed and burned Mediterranean shrubland of Southern Italy. *Ecosystems* 8, 182–190.
- Cipolli, F., Gambardella, B., Marini, L., Ottonello, G., Zuccolini, M.V., 2004. Geochemistry of high-pH waters from serpentinites of the Gruppo di Voltri

- (Genova, Italy) and reaction path modeling of CO₂ sequestration in serpentinite aquifers. *Appl. Geochem.* 19, 787–802.
- D'Alessandro, W., Bellomo, S., Brusca, L., Fiebig, J., Longo, M., Martelli, M., Pecoraino, G., Salerno, F., 2009. Hydrothermal methane fluxes from the soil at Pantelleria island (Italy). *J. Volcanol. Geotherm. Res.* 187, 147–157. <http://dx.doi.org/10.1016/j.jvolgeores.2009.08.018>.
- D'Alessandro, W., Brusca, L., Kyriakopoulos, K., Bellomo, S., Calabrese, S., 2014. A geochemical traverse along the “Sperchios Basin — evaikos Gulf” Graben (Central Greece): origin and evolution of the emitted fluids. *Mar. Pet. Geol.* 55, 295–308. <http://dx.doi.org/10.1016/j.marpetgeo.2013.12.011>.
- Daskalopoulou, K., D'Alessandro, W., Cabassi, J., Calabrese, S., Fiebig, J., Grassa, F., Kyriakopoulos, K., Parello, F., Tassi, F., 2016. Geochemistry of the gas manifestations of Greece: methane and light hydrocarbons. In: *Proc. of the 14th International Congress of the Geological Society of Greece*, May 25–27, 2016, vol. 50. Greece - Bulletin of the Geological Society of Greece, Thessaloniki. <http://hdl.handle.net/2122/10415>.
- Delichatsios, M.A., 1990. Procedure for calculating the air entrainment into turbulent pool and jet fires. *J. Fire Prot. Eng.* 2, 93–98.
- DesMarais, D.J., Donchin, J.H., Nehring, N.L., Truesdell, A.H., 1981. Molecular carbon isotopic evidence for the origin of geothermal hydrocarbons. *Nature* 292, 826–828.
- Dilek, Y., Thy, P., 2009. Island arc tholeiite to boninitic melt evolution of the Cretaceous Kizildag (Turkey) ophiolite: model for multi-stage early arc–forearc magmatism in Tethyan subduction factories. *Lithos* 113, 68–87. <http://dx.doi.org/10.1016/j.lithos.2009.05.044>.
- Etiopie, G., Sherwood Lollar, B., 2013. Abiotic methane on Earth. *Rev. Geophys.* 51, 276–299. <http://dx.doi.org/10.1002/rog.20011>.
- Etiopie, G., Schoell, M., 2014. Abiotic gas: atypical but not rare. *Elements* 10, 291–296.
- Etiopie, G., Ionescu, A., 2015. Low-temperature catalytic CO₂ hydrogenation with geological quantities of ruthenium: a possible abiotic CH₄ source in chromite-rich serpentinized rocks. *Geofluids* 15, 438–452. <http://dx.doi.org/10.1111/gfl.12106>.
- Etiopie, G., Lassey, K.R., Klusman, R.W., Boschi, E., 2008. Reappraisal of the fossil methane budget and related emission from geologic sources. *Geophys. Res. Lett.* 35, L09307. <http://dx.doi.org/10.1029/2008GL033623>.
- Etiopie, G., Schoell, M., Hosgörmez, H., 2011. Abiotic methane flux from the Chimaera seep and Tekirova ophiolites (Turkey): Understanding gas exhalation from low temperature serpentinization and implications for Mars. *Earth Planet. Sci. Lett.* 310, 96–104. <http://dx.doi.org/10.1016/j.epsl.2011.08.001>.
- Etiopie, G., Tsikouras, B., Kordella, S., Ifandi, E., Christodoulou, D., Papatheodorou, G., 2013a. Methane flux and origin in the Othrys ophiolite hyperalkaline springs, Greece. *Chem. Geol.* 347, 161–174. <http://dx.doi.org/10.1016/j.chemgeo.2013.04.003>.
- Etiopie, G., Vance, S., Christensen, L.E., Marques, J.M., Ribeiro da Costa, I., 2013b. Methane in serpentinized ultramafic rocks in mainland Portugal. *Mar. Pet. Geol.* 45, 12–16. <http://dx.doi.org/10.1016/j.marpetgeo.2013.04.009>.
- Etiopie, G., Judas, J., Whitticar, M.J., 2015. Occurrence of abiotic methane in the eastern United Arab Emirates ophiolite aquifer. *Arab. J. Geosci.* 8, 11345–11348.
- Etiopie, G., Vadillo, I., Whitticar, M.J., Marques, J.M., Carreira, P.M., Tiago, I., Benavente, J., Jimenez, P., Urresti, B., 2016. Abiotic methane seepage in the Ronda peridotite massif, southern Spain. *Appl. Geochem.* 66, 101–113. <http://dx.doi.org/10.1016/j.apgeochem.2015.12.001>.
- Etiopie, G., Klusman, R.W., 2010. Microseepage in drylands: flux and implications in the global atmospheric source/sink budget of methane. *Glob. Planet. Change* 72, 265–274.
- Evans, B.W., Hattori, K., Baronnet, A., 2013. Serpentinite: what, why, where? *Elements* 9 (2), 99–106.
- Fiebig, J., Hofmann, S., Tassi, F., D'Alessandro, W., Vaselli, O., Woodland, A.B., 2015. Isotopic patterns of hydrothermal hydrocarbons emitted from Mediterranean volcanoes. *Chem. Geol.* 396, 152–163.
- Fritz, P., Clark, I.D., Fontes, J.-C., Whitticar, M.J., Faber, E., 1992. Deuterium and 13C evidence for low temperature production of hydrogen and methane in a highly alkaline groundwater environment in Oman. In: *Kharaka, Y.K., Maest, A.S. (Eds.), Proceed. 7th Intern. Symp. On Water–rock Interaction: Low Temperature Environments*, vol. 1. Balkema, Rotterdam, pp. 793–796.
- Hanson, R.S., Hanson, T.E., 1996. Methanotrophic bacteria. *Microbiol. Rev.* 60, 439–471.
- Hirth, G., Guillot, S., 2013. Rheology and tectonic significance of serpentinite. In: *Serpentines* (Guillot, S., Hattori, K., eds.), *Elements* vol. 9(2), 107–113, doi: 10.2113/gselements9.2.107.
- Horibe, Y., Craig, H., 1995. D/H fractionation in the system methane–hydrogen–water. *Geochim. Cosmochim. Acta* 59 (24), 5209–5217.
- Hosgörmez, H., Etiopie, G., Yalçın, M.N., 2008. New evidence for a mixed inorganic and organic origin of the Olympic Chimaera fire (Turkey): a large onshore seepage of abiogenic gas. *Geofluids* 8, 263–275.
- Inguaggiato, S., Rizzo, A., 2004. Dissolved helium isotope ratios in groundwaters: a new technique based on gas–water re-equilibration and its application to Stromboli volcanic system. *Appl. Geochem.* 19, 665–673. <http://dx.doi.org/10.1016/j.apgeochem.2003.10.009>.
- Italiano, F., Sasmaz, A., Yüce, G., Okan, O.O., 2013. Thermal fluids along the East Anatolian Fault Zone (EAFZ): geochemical features and relationships with the tectonic setting. *Chem. Geol.* 339, 103–114.
- Italiano, F., Yüce, G., Uysal, I.T., Gasparon, M., Morelli, G., 2014. Insights into mantle-type volatiles contribution from dissolved gases in artesian waters of the Great Artesian Basin, Australia. *Chem. Geol.* 378–379, 75–88. <http://dx.doi.org/10.1016/j.chemgeo.2014.04.013>.
- Jin, Q., Xiong, S., Lu, P., 1999. Catalysis and hydrogenation: volcanic activity and hydrocarbon generation in rift basins, eastern China. *Appl. Geochem.* 14, 547–558.
- Liotta, M., Martelli, M., 2012. Dissolved gases in brackish thermal waters: an improved analytical method. *Geofluids* 12, 236–244. <http://dx.doi.org/10.1111/j.1468-8123.2012.00365.x>.
- Livingston, G.P., Hutchinson, G.L., 1995. Enclosure-based measurement of trace gas exchange: applications and sources of error. In: *Matson, P.A., Harriss, R.C. (Eds.), Biogenic Trace Gases: Measuring Emissions from Soil and Water. Methods in Ecology.* Blackwell Science Cambridge University Press, London, pp. 14–51.
- Mahmoud, Y., Masson, F., Meghraoui, M., Cakir, Z., Alchalbi, A., Yavasoglu, H., Yönlü, O., Daoud, M., Ergintav, S., Inan, S., 2013. Kinematic study at the junction of the East Anatolian fault and the Dead Sea fault from GPS measurements. *J. Geodyn.* 67, 30–39. <http://dx.doi.org/10.1016/j.jog.2012.05.006>.
- Mayhew, L.E., Ellison, E.T., McCollom, T.M., Trainor, T.P., Templeton, A.S., 2013. Hydrogen generation from low-temperature water–rock reactions. *Nature Geosci.* 6, 478–484.
- McCollom, T.M., 2007. Geochemical constraints on sources of metabolic energy for chemolithoautotrophy in ultramafic-hosted deep-sea hydrothermal systems. *Astrobiol.* 7, 933–950.
- McCollom, T.M., Bach, W., 2009. Thermodynamic constraints on hydrogen generation during serpentinization of ultramafic rocks. *Geochim. Cosmochim. Acta* 73, 856–875.
- McCollom, T.M., Seewald, J.S., 2013. Serpentinites, hydrogen, and life. In: *Serpentines* (Guillot, S., Hattori, K., eds.), *Elements* vol. 9, (2), 129–134, doi: 10.2113/gselements9.2.129.
- Miller, H.M., Matter, J.M., Kelemen, P., Ellison, E.T., Conrad, M.E., Fierer, N., Ruchala, T., Tominaga, M., Templeton, A.S., 2016. Modern water/rock reactions in Oman hyperalkaline peridotite aquifers and implications for microbial habitability. *Geochim. Cosmochim. Acta* 179, 217–241.
- Morrill, P.L., Gijs Kuenen, J., Johnson, O.J., Suzuki, S., Rietze, A., Sessions, A.L., Fogel, M.L., Nealson, K.H., 2013. Geochemistry and geobiology of a present-day serpentinization site in California: The Cedars. *Geochim. Cosmochim. Acta* 109, 222–240. <http://dx.doi.org/10.1016/j.gca.2013.01.043>.
- Mottl, M.J., Komor, S.C., Fryer, P., Moyer, C.L., 2003. Deep-slab fluids fuel extremophilic archaea on a mariana forearc serpentinite mud volcano: Ocean drilling program leg 195. *Geochim. Geophys. Geosystems* 4. <http://dx.doi.org/10.1029/2003GC000588>.
- Neal, C., Stanger, G., 1983. Hydrogen generation from mantle source rocks in Oman. *Earth Planet. Sci. Lett.* 66, 315–320. [http://dx.doi.org/10.1016/0012-821X\(83\)90144-9](http://dx.doi.org/10.1016/0012-821X(83)90144-9).
- Neubeck, A., Thanh Duc, N., Hellevang, H., Oze, C., Bastviken, D., Bacsik, Z., Holm, N.G., 2014. Olivine alteration and H₂ production in carbonate-rich, low temperature aqueous environments. *Planet. Space Sci.* 96, 51–61.
- Proskurowski, G., Lilley, M.D., Seewald, J.S., Früh-Green, G.L., Olson, E.J., Lupton, J.E., Sylva, S.P., Kelley, D.S., 2008. Abiogenic hydrocarbon production at Lost City hydrothermal field. *Science* 319, 604–607. <http://dx.doi.org/10.1126/science.1151194>.
- Potter, J., Rankin, A.H., Treloar, P.J., 2004. Abiogenic Fischer-Tropsch synthesis of hydrocarbons in alkaline igneous rocks; fluid inclusion, textural and isotopic evidence from the Lovozero complex, N.W. Russia. *Lithos* 75, 311–330. <http://dx.doi.org/10.1016/j.lithos.2004.03.003>.
- Power, I.M., Wilson, S.A., Dipple, G.M., 2013. Serpentinite carbonation for CO₂ sequestration. In: *Serpentines* (Guillot, S., Hattori, K., eds.), *Elements* vol. 9, (2), 115–121, doi: 10.2113/gselements9.2.115.
- Quatrini, P., Tagliavia, M., Gagliano, A.L., Yüce, G., D'Alessandro, W., 2016. Profiling microbial communities in hyperalkaline waters of the Kizildag ophiolite complex (Turkey). Abstract presented at the XIV Congress of the Italian Federation of Life Sciences (FISV) Rome, Italy 20–23 September 2016.
- Sanchez-Murillo, R., Gazel, E., Schwarzenbach, E., Crespo-Molina, M., Schrenk, M.O., Boll, J., Gill, B.C., 2014. Geochemical evidence for active tropical serpentinization in the Santa Elena Ophiolite, Costa Rica: an analog of a humid early Earth? *Geochim. Geophys. Geosyst.* 15, 1783–1800.
- Sano, Y., Wakita, H., 1985. Geographical distribution of ³He/⁴He in Japan: implications for arc tectonics and incipient magmatism. *J. Geophys. Res.* 90, 8729–8741.
- Schoell, M., 1980. The hydrogen and carbon isotopic composition of methane from natural gases of various origins. *Geochim. Cosmochim. Acta* 44, 649–661.
- Schrenk, M.O., Brazelton, W.J., Lang, S.Q., 2013. Serpentinization, carbon, and deep life. *Rev. Mineral. Geochem.* 75, 575–606. <http://dx.doi.org/10.2138/rmg.2013.75.18>.
- Sengör, A.M.C., Yılmaz, Y., 1981. Tethyan evolution of Turkey: a plate tectonic approach. *Tectonophysics* 75, 181–241.
- Seyfried, W.E., Foustoukos, D.I., Fu, Q., 2007. Redox evolution and mass transfer during serpentinization: an experimental and theoretical study at 200 °C, 500 bar with implications for ultramafic-hosted hydrothermal systems at Mid-Ocean Ridges. *Geochim. Cosmochim. Acta* 71, 3872–3886.
- Sherwood Lollar, B., Lacrampe-Couloume, G., Voglesonger, K., Onstott, T.C., Pratt, L.M., Slater, G.F., 2008. Isotopic signatures of CH₄ and higher hydrocarbon gases from Precambrian Shield sites: a model for abiogenic polymerization of hydrocarbons. *Geochim. Cosmochim. Acta* 72, 4778–4795. <http://dx.doi.org/10.1016/j.gca.2008.07.004>.
- Suda, K., Ueno, Y., Yoshizaki, M., Nakamura, H., Kurokawa, K., Nishiyama, E.,

- Yoshino, K., Hongoh, Y., Kawachi, K., Omori, S., Yamada, K., Yoshida, N., Maruyama, S., 2014. Origin of methane in serpentinite-hosted hydrothermal systems: The CH₄–H₂–H₂O hydrogen isotope systematics of the Hakuba Happo hot spring. *Earth Planet. Sci. Lett.* 386, 112–125. <http://dx.doi.org/10.1016/j.epsl.2013.11.001>.
- Szponar, N., Brazelton, W.J., Schrenk, M.O., Bower, D.M., Steele, A., Morrill, P.L., 2013. Geochemistry of a continental site of serpentinization, the tablelands ophiolite, gros morne national park: A mars analogue. *Icarus* 224, 286–296. <http://dx.doi.org/10.1016/j.icarus.2012.07.004>.
- Tekeli, O., Erendil, M., Whitechurch, H., 1983. The Kizildag ophiolite. In: autochthons, parautochthons and ophiolites of the eastern taurus and amanos mountains 1983. *Field Guideb.* 22–32.
- Tiago, I., Verissimo, A., 2013. Microbial and functional diversity of a subterrestrial high pH groundwater associated to serpentinization. *Environm. Microbiol.* 15 (6), 1687–1706.
- TUBITAK, 2015. Determination of Fault Activity and Geothermal Origin by Soil and Groundwater Degassing: The Extension of Dead Sea Fault Zone (DSFZ) in the Amik Basin (Hatay) and its Relation with Karasu Fault Zone and Origin of Thermal Waters in Amik Basin, TUBITAK-cost Research Project in the Frame of COST Action. Project No: 111Y090, Project Final Report, June 2015, p. 215 (in Turkish).
- Yüce, G., Italiano, F., D'Alessandro, W., Yalcin, T.H., Yasin, D.U., Gülbay, A.H., Ozyurt, N.N., Rojay, B., Karabacak, V., Bellomo, S., Brusca, L., Yang, F.T., Fu, C.C., Lai, C.W., Ozacar, A., Walia, V., 2014. Origin and interactions of fluids circulating over the Amik Basin (Hatay-Turkey) and relationships with the hydrologic, geologic and tectonic settings. *Chem. Geol.* 388, 23–39.